Local scale high frequency monitoring of seaweed strandings along an intertidal shore of the English Channel (Luc-sur-Mer, Normandy France) – Effect of biotic and abiotic factors

Stéphanie Lemesle, Anne-Marie Rusig, Isabelle Mussio

Local scale high frequency monitoring of seaweed strandings along an intertidal shore of the English Channel (Luc-sur-Mer, Normandy France) – Effect of biotic and abiotic factors

Stéphanie Lemesle [a], Anne-Marie Rusig [a,b], Isabelle Mussio [a,b*]

a-Laboratoire de Biologie des Organismes et Ecosystèmes Aquatiques (UMR 8067 BOREA), Muséum National d'Histoire Naturelle, CNRS, IRD, Sorbonne Université, Université des Antilles, Université Caen-Normandie, F-14032 Caen, France
b-Centre de Recherche en Environnement Côtier - Station Marine -Université de Caen-Normandie BP49, 54, rue du Docteur Charcot - 14530 Luc-sur-Mer

*Corresponding author
E-mail address: isabelle.mussio@unicaen.fr

1.Introduction

Sandy beaches worldwide are being affected by accumulations of beach-cast seaweeds and seagrasses exported from the surrounding ecosystems such as seagrass beds or rocky intertidal shores (MacLachlan and Brown, 2006). Once stranded on the beaches, macroalgae can provide a transitory habitat for several animal species including microorganisms and small invertebrates, often detritivores (Dugan et al., 2003; Orr et al., 2014). This allochthonous organic material is a significant source of food for intertidal and supratidal herbivore and decomposer communities (Orr et al., 2005) but also supplies higher trophic levels (Dugan et al., 2003; Fox et al., 2015; Mellbrand et al., 2011). The accumulation of wrack on beaches can also filter out wave effects, thereby reducing beach erosion (Ochieng and Erftemeijer, 1999). Moreover, by reflecting coastal marine biodiversity, beach wrack could be an interesting source of more easily accessible data on phytobenthic biodiversity (Suursaar et al., 2014, Lopez et al., 2019), in particular in the context of the Water Framework Directive (WFD, 2000/60/EC) in which the assessment of biological communities such as macroalgae is recognized as a quality indicator to evaluate the ecological status of water bodies (Panayotidis et al., 2004). Although the stranding of algae is a natural process, the imbalance in nutrients exported to the coastal zone increases this phenomenon both in intensity and in frequency. The increase of marine eutrophication observed over the past 30 years has led to excessive primary production characterised by phytoplankton blooms and/or the proliferation of opportunistic species which modify the structure of macroalgal assemblages (Kroeze et al., 2013; Morand and Merceron, 2004). The massive development of opportunistic macroalgae is therefore listed as a quality indicator in the European Water Framework Directive (WFD, 2000/60/EC).

Green macroalgae blooms occurring on the coast of Normandy (Bay of Seine) have been monitored by the French Algae Technology and Innovation (CEVA) since 2008 (Foveau et al., 2018) through aerial and ground-truthing surveys, but detailed studies of species composition and ecological studies are still rare. In contrast to ‘green tides’, in Normandy, large belts of green algae are attached to the rocky plateau along the foreshore before being detached and stranded under the influence of biological and physical factors.

The poor or bad ecological status of 31% of the coastal water bodies in the Bay of Seine is partially due to recurrent blooms of phytoplankton or macroalgae (AESN, 2020). Accumulations of seaweed interfere with human activities in coastal areas, particularly along the Normandy coast, which is composed of immense sandy beaches, a major tourist attraction.

The use of this stranded algal biomass is still limited. Exploiting this potential source of natural products (Mandalka et al., 2019) depends on stable access to raw material and knowledge of its availability and taxonomic diversity. To date, no qualitative and quantitative analyses of algal wracks in France are

reported in the literature and only a few studies are available worldwide (Piriz et al., 2003; Orr et al., 2005; Gómez et al., 2013; Suursaar et al., 2014; Villares et al., 2016; Cavalcanti et al., 2022).

While the 'green tides' in Brittany (France) and in other parts of the world have been well studied for several years (Teichberg et al., 2010; Diaz et al., 2013; Liu et al., 2013; Perrot et al., 2014; Schreyers et al., 2021) no data are available on the stranding dynamics along the coast of Normandy. In contrast to sheltered sites where blooms of opportunistic algae are often linked to nutrient inputs due to high water retention and higher seawater temperatures, in the open coastal area of Normandy, seaweed faces harsher living conditions due to wind and tidal effects. This physically dynamic habitat is colonised by specific seaweed assemblages, which are mainly structured by physical forces (Defeo et al., 2009). Hydrodynamic parameters in exposed coastal areas such as ocean currents, tides, winds and waves play a major role in the transport of free-floating or detached seaweeds and their accumulation on beaches (Biber, 2007; Gómez et al., 2013; Suursaar et al., 2014; Orr et al., 2014; López et al., 2019). The supply of wrack along the coast of Normandy can also vary considerably depending on environmental drivers like temperature, the impact of light on the growth of algae and the stock of algae on the rocky shore. Seasonal variations and the interactions between these environmental factors are also known to influence the growth and physiology of macroalgae (Altamirano et al., 2000; Barr et al., 2008). Other control factors may be involved such as complex intra- and interspecific interactions between macroalgae and competition for colonisation of the rocky substrate. Schreiber et al. (2020) noted that the link between benthic populations and stranded seaweeds has received little attention. The complexity of these biotic and abiotic drivers makes it difficult to predict temporal patterns of stranded seaweed biomass (López et al., 2019) and consequently to assess the risk of the development of algal bloom and to design coastal management strategies.

To better understand the characteristics and the dynamics of algal wracks on the Normandy coast, the specific aims of the study were to 1) assess the temporal dynamics of macroalgal wracks through high frequency monitoring, and their links with environmental conditions, 2) test the hypothesis of the local origin of these deposits by comparing the flora on the neighbouring rocky shore with the composition of the wrack and 3) describe the role of variations in hydrodynamics on the formation of beach wrack in an exposed coastal site.

2.Materials and methods

2.1 Study site

The study was conducted at Luc-sur-Mer (Normandy, France), a seaside resort and tourist town (49°19’08’’N; 0°21’03”W) located on the west coast of the Bay of Seine in the English Channel. The coastline of Luc-sur-Mer is characterised by a large sandy area about 240 m wide followed by a large slightly sloping rocky plateau (1.5-2 km in width) colonised by seaweeds. The maximum depth on the foreshore does not exceed -15 m relative to hydrographic zero. The site is an open system oriented north-east with a macrotidal regime, semidiurnal with a maximum tidal amplitude average of 6.5 m during spring tide and 2.5 m during neap tides. Tidal currents are generally moderate, ranging between 0.8 and 1 $m.s^{-1}$ during maximum flood and ebb spring tide, and 90% of waves are less than 1.25 m in height (Dauvin, 2012). The English Channel is at the interface of the warm-temperate Atlantic oceanic system and the boreal North Sea and Baltic Sea continental systems of northern Europe (Dauvin, 2012).

2.2 Sampling of stranded seaweeds

To describe algae stranding dynamics, field sampling was carried out during low tide once or twice a week from March 2017 to October 2018. The extent of algal wrack (in hectares, Ha) was obtained by using GPS to delimit and record the position and the shape of the beaching zones along a 2-km beach line representing a total surface area of 30 Ha. The user positions around the stranding area were recorded at 5-second intervals with a Trimble TDC 100 GPS linked to a GPS enabled mapping software (Arpentgis mobil). The non-delimited beach zones were considered as having no stranded seaweed or having overly dispersed patches of wrack. Six quadrats randomly located within the delimited seaweed stranding zones were used to identify the species composition, cover and biomass of stranded algae. Total macroalgae abundances and specific composition were assessed by visually estimating their percentage cover in 0.25 m² quadrats, according to the Braun-Blanquet cover abundance scale (1951). The average cover value among quadrats was then calculated using the median points of each interval of the Braun-Blanquet scale data as follows (none=0; + very sparse=0.1; <5%=2.5; 5%-25%=15; 25%-50%=37.5; 50%-75%=62.5; 75%-100%= 87.5). Wrack species were determined to the lowest taxonomic level possible in the field. On each sampling occasion, the total surface area of algal wrack was corrected using the average cover of all macroalgae determined based on the quadrats. In each of six quadrats, the biomass of algal wrack was measured directly in the field with a digital dynamometer. Macroalgae were shaken to remove the sand and wet weights were recorded. If the wet weight was less than 100 g, the algae were transported to the laboratory in labelled plastic bags for weighing with an analytical balance. The fresh biomass of algal wrack was standardised to kilogram (fresh weight) per square metre (kg/m²). The monthly algal wrack biomass and coverage values were obtained by

calculating the mean of the field data collected each months during the monitoring of seaweed stranding (with N ranging from 3 field studies in March 2017 to 9 in September and August 2018).

2.3 Dynamics and diversity of seaweeds on the intertidal rocky shore

The dynamics of benthic algal vegetation of the rocky shore was analysed in spring, summer, autumn in 2017-2018 and in winter 2018 during low tide. Fieldwork was based on the sampling method developed by Cosson and Thouin (1981). Three 260-m transects were selected perpendicular to the coast and divided into segments (n=8 to 11 segments). The length of each segment depended on variations in algal cover, specific composition and geomorphological characteristics. The lengths ranged from 10 m (heterogeneous areas) to 80 m (homogenous areas). A minimum distance of 30 m between transects was applied. All algal species observed along the 2-m-wide transect in each segment were identified and recorded using the Braun-Blanquet cover-abundance scale. Macroalgae were identified *in situ* to species level, and if necessary taken to the laboratory for identification under the microscope. The nomenclature was checked against Guiry and Guiry (2020: www.algaebase.org). The functional form of each seaweed species recorded in the beach wracks and on the rocky shore was identified according to the classification of Blomqvist et al. (2014). Species richness of rocky shores was recorded as the average number of total species, and mean number of Rhodophyceae, Phaeophyceae and Ulvophyceae and abundance (total mean cover of vegetation and mean cover of Rhodophyceae, Phaeophyceae and Ulvophyceae) were calculated for each transect.

2.4 Environmental data

Meteorological data for the years 2017 and 2018 (air temperature (°C), solar radiation (J cm^{-2})), wind forcing (speed (m s^{-1}) and direction (°)) were obtained from Bernières-sur-Mer meteorological station located 6 km to the west of the study site (Météo-France data). The significant wave height (SWH, average height of the 1/3 highest waves) and the tidal current (TC, m/s) were obtained from the CREC marine station (University of Caen-Normandie) located at Luc-sur-Mer using a VALEPORT MIDAS current meter positioned in front of the marine station at the lower limit of the low spring tides (49°19'16.11"N; 0°20'53.22"W). The tidal amplitude forecast for Luc-sur-Mer was provided by the French Naval Hydrographic and Oceanographic Service (SHOM) and was chosen as being representative of tidal influence.

2.5 Statistical analysis

Shapiro and Wilk's tests were used to check the normal distribution and homogeneity of the data. In some cases, data were log10 transformed to meet the required criteria. To test the temporal variability of the beach wrack area, two-way ANOVA were performed using SigmaPlot 12.5 when normality and homoscedasticity were verified. The factors considered were years (2017 and 2018) and

months. A pairwise multiple comparison test (the Holm-Sidak method) was conducted if differences were observed between factors.

To determine the time-scale variability of the composition of the wrack species, statistical analyses were performed using the vegan package in R with XLSTAT-2019 software. Permutational multivariate analysis of variance (PERMANOVA) using Bray-Curtis distance matrix (Anderson, 2005) on square-root transformed abundance data was also performed to test the hypothesis that algal composition differed with the month/year and surface area of stranded seaweed.

The temporal variability of species richness and the total cover of benthic macroalgae on the rocky shore were analysed using one-way analysis of variance (ANOVA) to test for significant differences among sampling occasions. The Holm-Sidak post-hoc test was used when a significant difference was observed ($p < 0.05$). These statistical tests were performed using Sigmaplot 12.5.

Spearman's correlations were performed using Sigmaplot 12,5 (Systat Software Inc.) to identify the relationships between the extent of wrack and environmental variables. To perform these correlations, the total surface areas of stranded seaweed measured at each sampling occasion were used. Four classes of seaweed beaching were defined according to stranding area: negligible (<1 Ha); small (between 1 and 2.5 Ha); moderate (between 2.5 and 4.5 Ha) and high (> 4.5 Ha). Meteorological variables (air temperature and solar radiation) were calculated as the median daily value of the three days preceding sampling. The maximum tidal current (TCmax) measured 24 hours before the stranding event was used and the median value of the significant wave height was calculated using the measurement taken 24 hours before each sampling occasion. In the same way, for the wind conditions, the mean wind speed measured 24 hours before each sampling occasion and the dominant wind direction were used. The combined influence of wind speed and wind direction on waves and beach wrack areas was determined using the pollution rose available in the R openair package (Carslaw and Ropkins, 2012).

3. Results

3.1 Temporal variability of stranded surfaces and biomasses

From March 2017 to October 2018, seaweed strandings were evaluated on average once a week giving a total of 99 field surveys (Fig. 1). The mean surface area of stranded algal biomass varied markedly depending on the week with a seasonal trend that resulted in an increase in spring and summer and a decrease in autumn and winter. The biggest surface area, 98 hectares (±2.22 SD) of stranded seaweeds was observed on the 7th of September 2017. About 50% of patches of stranded seaweed were less than one hectare in size and were observed throughout the study period, in contrast to areas of stranded seaweed extending more than four hectares, which were rarely recorded and more frequently in the spring and summer months. Significant differences in the mean surface area of stranded seaweed were observed between months (ANOVA, $F(11) = 7.006$, $P < 0.001$) highlighting its seasonal variability. Moreover, in the most productive period (March to September), significant differences were observed between the two years (ANOVA, $F(1) = 12.265$, $P = 0.001$) and more specifically in June and July when significant differences ($P < 0.05$) were observed according to the Holm-Sidak method for pair-wise multiple comparisons. In fact, a major increase in seaweed strandings was measured as early as June in 2017 but only in August in 2018 (Fig. 1A).

The average monthly value of stranded algal biomass ranged from 0.3±0.3 kg fresh wt m^{-2} in March 2018 to 3.4±2.3 kg fresh wt.m^{-2} and August 2017. The total amount of stranded seaweed was estimated at around 2,420 tonnes fresh weight in 2017 and around 1,709 tonnes fresh weight in 2018 during the growing season (April to October) in the study area in both years. The biomass of stranded seaweed followed similar seasonal trends as their surface area with highest biomass peak recorded in spring and summer, then declining in the winter months. Similarly, biomass peaks of more than 3 kg fresh wt.m^{-2} were observed from April to October in 2017 but only in August in 2018; biomass declined in late November and early December from a mean value generally below 2 kg fresh wt.m^{-2} (Fig. 1B).

3.2 Temporal variability of algal wrack composition

A total of 47 taxa of macroalgae (14 Phaeophyta, 28 Rhodophyta, and 5 Chlorophyta) were identified in algae strandings from March 2017 to October 2018 (Tab. 1). Twenty-nine taxa had a mean cover > 0.5% and amongst these taxa, 9 were dominant with a mean cover >2% (Appendix). Figure 2 shows the monthly proportion of these dominant species and highlights the largest contribution of the genus *Ulva* spp. (Ulvophyceae) and of the perennial brown algae *Fucus serratus* (Fucaceae) in the composition of algal wracks. Counting all the seaweed strandings recorded, the mean proportion of *Ulva* sp. (Ulvales) represented more than 50% of the total beach wrack. This taxon was dominant in spring and summer, except in June and July 2018, when large brown algae such as *Saccharina latissima*

(Laminariales) or *Sargassum muticum* (Fucales) were abundant. Like *Ulva* spp. the perennial brown algae *Fucus serratus* (Fucales) was also abundant in the algal wracks and was generally present in all wracks sampled. Large strandings of *Laminaria digitata* (Laminariales) were mainly observed in late summer and from September 2017 to March 2018. Amongst Rhodophyta species, *Plocamium cartilagineum* (Plocamiales) was the species the most often present in wracks (from October 2017 to February 2018) while *Ceramium rubrum* (Ceramiales) and *Cryptopleura ramosa* (Ceramiales) were present in most samplings but usually with a low mean proportion, often < 10%. The frequency of other species varied with the season.

PERMANOVA analysis of the specific composition of stranded seaweeds with a mean cover value > 0.5% recorded on at least one sampling date revealed a significant influence of the factors "Extent of algal wrack", "Year" and "Months". Significant interaction between "Month" and "Year" was also found. Species composition of macroalgal wracks differed over time due to seasonal variation and depending on the size of the wrack deposition (Tab. 2). The same analysis of variance limited to the most productive period (from March to September) also revealed significant differences between "Years" (PERMANOVA, year, $p = 0.001$), "Months" (PERMANOVA, months, $p < 0.001$) and combination of "Months" and "Years" (PERMANOVA, Months x Year, $p = 0.002$). Wrack composition differed significantly between the two years in June ($p < 0.001$, Holm's test) and in July ($p < 0.001$, Holm's test).

3.3 Temporal variability of the composition of rocky shore species

A total of 35 taxa of macroalgae (8 Phaeophyta, 23 Rhodophyta, and 4 Chlorophyta) were identified on the rocky shore (Tab. 1). The highest total average percentage cover was observed in spring and summer 2017 with respectively 59±3% and 54±4%, and in autumn 2018 (55±3%), while the total average percentage coverage was lowest (17±1%) in winter 2018 (Fig. 3A). A significant decrease in macroalgae coverage was observed between growing seasons (Spring 2017) and Winter 2018 (ANOVA, $F = 5.15$, $P = 0.005$). Brown algae had the highest coverage on the rocky shore, often accounting for more than 40% of the total vegetation coverage in particular in winter 2018 (68%). The percentage coverage of Ulvophyceae was often > 30% with the highest value in summer 2018 (50%) and the lowest (7%) in winter 2018. The coverage of red algae was relatively stable throughout the sampling period, close to 20% (Fig. 3A). The total average species richness on the rocky substrate ranged from 24(±2) in spring 2017 to 12(±3) in winter 2018 with significant differences (ANOVA, $F = 5.08$, $P = 0.006$). The proportion of taxonomic richness of Rhodophyceae (> 47%) was higher than that of Phaeophyceae and Ulvophyceae, the latter represented no more than 25% of the taxonomic richness of the rocky shore (Fig. 3B).

3.4 Comparison of the species composition on the rocky shore and in the algal wracks

Table 1 summarises the species recorded in the seaweed strandings (table column BW) and on the closest rocky shore (table column RS). Amongst the 47 taxa identified in wrack deposits, 29 were also identified on the rocky shore. Species characteristics of the midlittoral zone were well represented in the wracks and on the rocky shore corresponding to the following taxa: *Dictyota dichotoma* (Dictyotales), *Fucus serratus* (Fucales), *Fucus vesiculosus* (Fucales), *Saccharina latissima* (Laminariales), *Sargassum muticum* (Fucales), *Ceramium rubrum* (Ceramiales), *Chondrus crispus* (Gigartinales), *Cryptopleura ramosa* (Ceramiales), *Cystoclonium purpureum* (Gigartinales), *Dilsea carnosa* (Gigartinales), *Gracilaria gracilis* (Gracilariales), *Palmaria palmata* (Palmariales) and *Ulva* sp. (Ulvales). Six species belonging to Rhodophyta were only observed on the rocky shore and 18 seaweed species as well as Rhodophyta (11 taxa), Chlorophyta (1 species) and Phaeophyta (6 species) were only observed in the strandings.

Concerning the classification of seaweeds in functional groups (see Table 1, column 'Functional group'), most of the seaweeds observed on rocky substrate belonged to the leathery group (e.g. *Fucus* spp, *S. muticum* or Laminarian), and accounted for the highest percentage (39%) followed by the foliose group (30%) (Fig.4). The filamentous and the corticated foliose groups had similar percentages of around 13%. Algae strandings were composed of a mixture of leathery taxa, foliose species (e.g. *Ulva* sp.), filamentous algae (e.g. *C. rubrum*) and corticated foliose species (e.g. *D. dichotoma* or *C. crispus*). The leathery and foliose groups showed the highest values with 42% and 34% respectively. In the same way, corticated foliose and filamentous seaweeds were occasionally found on wrack samples at 11% and 9% respectively. The thick soft and hard corticated groups were present at the smallest percentages, i.e. less than 2%. Crustose algae, which were sparse on the rocky shore (0.5%) were not found in the stranded seaweeds at all.

3.5 Abiotic factors that affect seaweed strandings

To characterise the marine meteorological conditions leading to the strandings classified as large scale (> 4.5 Ha), wind speed and tidal threshold (forecast tide height) were defined 24 hours before each stranding event. Among the 47 seaweed strandings recorded from June to October in 2017 and from August to October in 2018, 23% were classified as large, 34% as moderate, 29% as small and 12% as negligible. Figure 5 shows that large wrack deposits mainly occurred during the growing season when wind speed was > 2.6 m s^{-1} and the predicted tide height was > 6.8 m. Among the 11 wrack deposits classified as large scale, only one tide height was less than 6.8 m. Thus, in the growing season, bigger algal strandings were recorded during spring tides than during neap tides (ANOVA; n = 26; F1.2 = 8.0122; p = 0.006). In contrast to the forecast tide height, wind speed during large scale strandings was more variable, ranging from 2.6 m s^{-1} to 5.6 m s^{-1}.

A positive and significant Spearman's correlation was found between air temperature and the extent of beach-wracks areas measured throughout the sampling period and growing seasons (spring and summer) with r = 0.52 and r = 0.42, respectively (Tab. 3). A significant direct correlation was also observed with significant wave height (r = 0.27) and a negative correlation with solar radiation (r = -0.24) in the growing seasons. In contrast, no significant correlation was found between the extent of the wrack and other physical variables (wind speed and maximum tidal current).

The speed and direction of the wind measured at the Bernières-sur-Mer meteorological station in the spring and summer of both years are presented in figure 6A. During this sampling period, the prevailing winds were from the west-south-west (WSW) and from the north-north-east (NNE), mostly at a velocity > 4 $m.s^{-1}$, respectively 67% and 60% of the time. Figure 6B shows that the highest significant wave heights (> 0.3m) were again mostly associated with WSW and the NNE wind directions and, like the wind regime, less frequently with the west (W) and the north-east (NE) wind directions. When winds blew from the WSW, 30% of waves were > 0.3m in height, while NNE winds generated 44% of waves > 0.3m. A linear correlation was observed between wind speed (regardless of direction) and significant wave height (r = 0,39, P < 0.0001, y = 0.0689x – 0.0139, n = 465). Figure 6C shows that the biggest beach wracks (>4.5 Ha) were associated with the WSW (38% of beach wracks), SSW (26%), W (18%) and NNE (10%) winds.

3.6 Meteorological conditions during the sampling period (April 2017-October 2018)

To understand why seaweed strandings occurred later in summer 2018 than in 2017, interannual comparisons of meteorological parameters (solar radiation and air temperature) were performed and the results are listed in table 4. Concerning air temperatures, in 2017 spring started earlier than in 2018 with temperatures above 15°C already recorded in March. This seasonal shift was very clear in May when daily temperatures > 15°C were measured during 45% of the month in 2017 compared to in only 19% in 2018. In both years, April was a key month with respect to the quantity of light available for seaweed growth. In 2017, 5 days (16%) with solar radiation >1300 J/cm² were recorded in March with an increase to 25 days (83%) in April. In 2018, the quantity of light received by the seaweeds each day was lower, as only 2 days (6%) in March had radiation >1300 J/cm² and 14 days (47%) in April. The average percentage of days with solar radiation > 1300 J/cm² was balanced in the summer months of both years.

4. Discussion

High frequency monitoring of wrack deposits highlighted marked temporal variability (inter- and intra-annual) in terms of stranded biomass, extent of the strandings, and seaweed composition. The magnitude of these seaweed strandings was similar to those quantified in other open sea zones (Piriz et al. 2003, Villares et al. 2016). During the growing season, the genus *Ulva* (Ulvales) predominated wrack species composition thereby confirming the existence of blooms of opportunistic algae in the water at our study site. However, unlike in sheltered bays in Brittany where monospecific *Ulva* strandings reaching 8000 to 12000 tonnes year^{-1} of *Ulva* have been regularly observed (Merceron, 1999; Schreyers et al., 2021), the wrack species comprised a mixture of Phaeophyceae, Ulvophyceae and Rhodophyceae even during summer strandings. Thus, in contrast to monospecific stranding events of macroalgae which are often linked to coastal water eutrophication (Perrot et al. 2014; Teichberg et al. 2010; Diaz et al. 2013; Liu et al. 2013; Merceron et al., 2007), the magnitude and species composition of stranded seaweeds in this study seem to depend on a number of biotic and abiotic factors thus rendering the link with nutrient enrichment more complex.

The occurrence of high peaks of seaweed strandings mainly between June and October is clearly linked to the growing season of many annual species of seaweeds in the Bay of Seine. The results of the comparison of algal diversity of the wracks and of the rocky shore suggest that the stranded macroalgae are of local origin and that biotic factors such as the natural succession of seaweed assemblage and the specific life cycle of each algal species have an impact on wrack accumulation dynamics (Barreiro et al. 2011). At our study site, rocky shores and wrack deposits were dominated by brown algae (e.g. *Fucus serratus*, *Saccharina latissima* and *Sargassum muticum*) whereas taxonomic richness was mainly represented by Rhodophyceae. The ratios of red to brown and of red to green algae in wrack deposits were similar to those observed on the nearby rocky shore. The composition of seaweed strandings was shown to reflect the benthic populations, almost 83% of species present on the nearby rocky shore were also recorded in strandings. Moreover, the proportions of the different functional groups of seaweed in the beach wrack (mainly leathery, foliose, corticated foliose and filamentous algae) were quite close to those recorded on the rocky shore. Other studies have also reported a relationship between stranded seaweeds and adjacent benthic algae populations (Schreiber et al., 2020, López et al., 2017). About half the species recorded in the wrack deposits are characteristic of the exposed midlittoral, and some form belts. Species only observed on the rocky shore included crustose algae firmly anchored to the substrate (*Hildenbrandia rubra*, *Lithophyllum incrustans*, *Lithothamnion lenormandii)* or species forming poor benthic populations. Most of the species not recorded on the rocky shore lived in the subtidal zones, these included *Apoglossum ruscifolium* (Ceramiales), *Dasya corymbifera* (Ceramiales), *Heterosiphonia plumosa* (Ceramiales), *Kallymenia*

reniformis (Gigartinales) or *Callophyllis laciniata* (Gigartinales) often epiphytic on *Laminaria* and *Umbraulva olivascens* (Ulvales). Other studies have also shown that the species composition of beach cast-seaweed may reflect the neighbouring subtidal flora diversity (López et al., 2019; Cavalcanti et al., 2022). Some species characteristics of sheltered coastal habitats were recorded sometimes in the wracks (*Ascophyllum nodosum*, *Himanthalia elongata* and a particular morphotype of *Sargassum muticum*) suggesting a more distant origin. Highly buoyant large brown macroalgae like Fucales *Sargassum* or *Ascophyllum* have long-distance dispersal ability and may thus be stranded many thousands of kilometres from their place of origin (Garden et al., 2015), also reported for another Fucale, *Durvillea antarctica* (Fraser et al., 2018; López et al., 2019). Thus, even if a high proportion of the detached macroalgae in our study appear to be of local origin; the exposed situation of the site makes it more vulnerable to inputs of drift material from surrounding areas compared to sheltered sites, as already described by Berglund et al. (2003).

Monthly qualitative assessment of the wrack revealed a slight predominance of leathery perennial brown seaweeds in winter and of annual green seaweeds in spring and summer. This shift between brown and green macroalgae is in agreement with the results of other studies whose authors attributed it to the differential growth strategies of perennial and annual species (Thakur et al. 2008, Gómez et al. 2013). In winter, the composition of wrack species was dominated by leathery and perennial algae (e.g. *Fucus serratus*, *Saccharina latissima* and *Laminaria digitata*) and by their epiphytes (e.g. *Plocamium cartilagineum*), probably due to more intense and frequent storm events at this period, contributing to their uprooting and drifting onto the beach. In the same way, the peak deposits of beach wrack observed in late summer and early autumn were mainly composed of brown *L. digitata* and *S latissima* and annual seaweeds (*Ulva* sp. and *Dictyota dichotoma*) and can be attributed to senescence and die-back stage of many seaweeds, which are consequently more easily uprooted by any wave action. Extensive seaweed beachings occurring at the tail end of the seaweed growth period in late summer have also been reported in other studies (Thakur et al., 2008; Barreiro et al., 2011; López et al., 2019).

Our field surveys showed that the rocky shore was dominated by algal species with morphologically simple forms (e.g. filamentous, foliose, corticated foliose algae) whereas perennial forms were very poorly represented. This can be explained by the environmental traits of the coastline such as sediment instability. The presence of soft (sand) and unstable (gravel and pebble) substrates on the rocky shore may reduce the development of sustainable macroalgal communities while benefiting opportunistic benthic algae such as *Ulva*. Thus differences in temporal variability throughout the annual cycle characterised by a more homogenous distribution of beach wrack in 2017 (from June to October) than in 2018 (mainly in August and September) are probably linked with the growth of annual species on

405 the rocky shore. In this sense, it is noteworthy that *Ulva* sp, which predominated in spring and summer,
406 was generally scarce in June and July 2018. Changes in environmental conditions between the two
407 years could explain the distinct dynamics of the variability of beach wrack events.

408 The significant positive correlation observed between air temperature and the extent of the beach
409 wracks supports this seasonal process. However, this effect was particularly marked during the
410 growing seasons, with a direct impact on the development of annual species and hence on the
411 occurrence and abundance of beach wracks. The productive period started later in 2018 than in 2017
412 due to a colder spring and to less favourable light conditions. These contrasted meteorological
413 conditions may explain the high algal cover on the rocky shore in spring 2017 and the significant algal
414 strandings from the beginning of summer 2017 compared to those in 2018.

415 Surprisingly, a negative correlation was found between solar radiation and the extent of the wrack
416 recorded during the growing seasons. Regardless of light availability, macroalgal production is also
417 limited by the reduction in light in highly turbid coastal waters (Ren et al. 2014), especially in highly
418 dynamic systems. The turbidity of the seawater along the coast of the eastern channel is high due to
419 the resuspension of soft bottom sediments and the influence of both terrestrial inputs from the River
420 Seine and of numerous small coastal rivers (Delebecq et al., 2013).

421 As our study site was an open environment, other parameters including waves and tidal effects must
422 also be considered as they create harsh living conditions for benthic macroalgae and contribute to
423 their drifting on to the beach. The period with the strongest effects in the Bay of Seine is between
424 October and March caused by strong winds and storm events. As already mentioned, in winter,
425 seaweed assemblages in our study site were dominated by perennial species whereas in spring and
426 summer, assemblages were largely dominated by annual and opportunistic species with a soft and
427 fragile thallus more sensitive to wave actions.

428 Major beach wrack events (> 4.5 Ha) were mainly observed when average wind speed measured 24 h
429 before the event was greater than 2.6 $m.s^{-1}$ and the forecast tide height was greater than 6.8 m.
430 However, the two thresholds alone are not sufficient to distinguish between the different types of algal
431 strandings, suggesting that other factors contribute to the intensity and frequency of the
432 phenomenon. We also recorded the majority of the stranded macroalgae areas during the spring tides
433 in agreement with reports by Ochieng and Erftermeier (1999) and Orr et al. (2005). But in contrast to
434 the study by Orr et al. (2005), tidal currents seemed to have no significant influence on wrack
435 accumulation, as the average tidal current recorded 24 h before the beach wrack event during our
436 sampling period did not exceed 0.3 $m.s^{-1}$ even during spring tides. Thakur et al. (2008) estimated that

437 uprooting and subsequent strandings of seaweeds occurred when the speed of the tidal current was
438 greater than 2 $m.s^{-1}$.

439 Waters in the English Channel are also likely to be influenced by turbulence caused by wind-generated
440 surface-gravity waves. The effects of these waves may lead to sediment being resuspended throughout
441 the water column, particularly in the western channel (van der Molen et al. 2009; Rivier et al. 2012)
442 explaining the significant linear correlation between wind speed and significant wave height observed
443 in the study ($R = 0.39$, $P < 0.0001$). Based on this observation, we hypothesise that winds may be the
444 main driving force behind beach wrack dynamics. Our results revealed no significant correlation
445 between wind speed and wrack deposition. The direction of the winds and the orientation of the coast
446 also have a significant impact on the effect of the prevailing winds and their strength on the
447 accumulation of wrack on the beach. The wind rose we obtained shows the dominance of winds from
448 a south-westerly to a westerly window, roughly parallel to the study site. These dominant westerly
449 winds (the main direction in the English Channel; Météo-France 1991) can cause a high energy wave
450 level and were also associated with large-scale accumulation of wrack macroalgae on the beach.
451 Indeed, around 80% of the beach wracks which extended more than 4.5 Ha were associated with these
452 dominant westerly winds. Extensive beach wracks were also associated with winds blowing from the
453 north-north-east. Stronger winds in spring and summer were associated with these winds
454 perpendicular from the coast which may generate maximum wave height (> 0.3 m). Larger wrack
455 deposits were also reported by Lastra et al. (2014) when sea wind blew perpendicular to the shore.
456 Thus during the growing season, the positive correlation between the daily average of the significant
457 wave height measured in the intertidal zone before the beach wrack event and when the wrack was
458 deposited seems to sustain the effect of the sea wind on the wrack dynamics. However, the weak
459 correlation shows that among these winds, westerly and north-northeast winds were the most able to
460 generate strong wave energy. An additional contribution comes from the currents produced by the
461 tides, which, when associated with sea winds, can cause uprooting of seaweeds.

462

5. Conclusion

In this study, we monitored the qualitative and quantitative variability of the pattern of wrack benthic macroalgae deposits and showed algal deposits in spring and summer were dominated by sheet-like and annual species, mainly represented by the genus *Ulva*, which is often considered as a symptom of anthropogenic pressure. Further studies are needed of seasonal strandings of fast-growing species which have a high potential to form massive blooms and of the link with the risk of eutrophication of coastal waters.

Our use of high frequency field observations underlined the need to use different time scales to explain temporal variations in wrack deposits at a short time scale (several hours before the stranding event) to account for the physical factors such as wind speed, wind direction and the tide on the one hand, and at a longer time scale to account for environmental parameters such as light intensity, air temperature and their seasonal interaction, on the other hand.

This work also underlines the difficulty of producing a predictable scenario of large-scale wrack deposits and the need to produce more data to develop predictive models for coastal seaweed strandings, which are needed both to make use of the stranded alga biomass and for the design of coastal management strategies.

ACKNOWLEDGMENTS

This study is part of the project “Study of the macroalgal heterospecific strandings along the Normandy coastline (Bay of Seine)” and was supported by the Seine-Normandy Water Agency (AESN) and the Normandy Region. The authors are grateful to all technical staff of the Coastal Environment Research Centre – Marine Station of the University of Caen Normandie (Luc-sur-Mer) for their assistance.

485 **REFERENCES**

486 AESN (2020) Etat des lieux 2019 du Bassin de la Seine et des cours d'eaux côtiers normands. 200pp

487 Anderson, M.J., 2005. PERMANOVA: a FORTRAN computer program for permutational multivariate
488 analysis of variance. Department of Statistics, University of Auckland, New Zealand. 24 pp.

489 Altamirano, M., Flores-Moya, A., Conde, F., Figueroa, F.L., 2000. Growth seasonality, photosynthetic
490 pigments, and carbon and nitrogen content in relation to environmental factors: a field study of *Ulva*
491 *olivascens* (Ulvales, Chlorophyta). Phycologia 39, 50-58.

492 Barr, N.G., Kloeppel, A., Rees, T.A.V., Scherer, C., Taylor, R.B., Wenzel, A., 2008. Wave surge increases
493 rates of growth and nutrient uptake in the green seaweed *Ulva pertusa* maintained at low bulk flow
494 velocities. Aquat. Biol. 3, 179-186.

495 Barreiro, F., Gómez, M., Lastra, M., López, J., de La Huz, R., 2011. Annual cycle of wrack supply to sandy
496 beaches: Effect of the physical environment. Mar. Ecol. Prog. Ser. 433, 65–74.

497 Berglund, J., Mattila, J., Rönnberg, O., Heikkilä, J., Bonsdorff, E., 2003. Seasonal and inter-annual
498 variation in occurrence and biomass of rooted macrophytes and drift algae in shallow bays. Est. Coast.
499 Shelf Sci. 56, 1167–1175.

500 Biber, P., 2007. Hydrodynamic transport of drifting macroalgae through a tidal cut. Est. Coast. Shelf Sci.
501 74, 565-569.

502 Blomqvist, B., Wikström, S.A, Carstensen, J., Qvarfordt, S., Krause-Jensen, D., 2014. Response of coastal
503 macrophytes to pressures. Deliverable 3.2-2, WATERS Report no. 2014:2 Havsmiljöinstitutet, Sweden.

504 Braun-Blanquet, J., 1951. Plant Sociology: the study of Plant Communities. McGraw Hill, New York.

505 Carslaw, D.C., Ropkins, K., 2012. Openair - An R package for air quality data analysis. Environ. Modell.
506 Software 27–28, 52–61.

507 Cavalcanti, M.I.L.G., Gonzalez Sanchez, P. M., Fujii, M.T. 2022. Comparison of the diversity and biomass
508 of beach-cast seaweeds from NE and SE Brazil. Eur. J. Phycol. DOI: 1080/09670262.2021.2003867

509 Cosson, J., Thouin, F., 1981. Etude du macrophytobenthos en baie de Seine : problèmes
510 méthodologiques. Vie Milieu 31, 113-118.

511 Dauvin, J.C., 2012. Are the eastern and western basins of the English Channel two separate
512 ecosystems? Mar. Pollut. Bull. 64, 463–471.

513 Defeo, O., McLachlan, A., Schoeman, D.S., Schlacher, T.A., Dugan, J., Jones, A., Lastra, M., Scapini, F.,
514 2009. Threats to sandy beach ecosystems: a review. Est. Coast. Shelf Sci. 81, 1-12.

515 Delebecq, G., Davoult, D., Menu, D., Janquin, M.A., Dauvin, J.C., Gevaert, F. 2013. Influence of local
516 environmental conditions on the seasonal acclimation process and the daily integrated production
517 rates of *Laminaria digitata* (Phaeophyta) in the English Channel. Mar. Biol. 160, 503–517.

518 Diaz, M., Darnhofer, I., Darrot, C., Beuret, J.E. 2013. Green tides in Brittany: What can we learn about
519 niche–regime interactions? Environ. Innov. Soc. Transit. 8, 62–75.

Dugan, J.E., Hubbard, D.M., McCrary, M.D., Pierson, M.O., 2003. The response of macrofauna communities and shorebirds to macrophyte wrack subsidies on exposed sandy beaches of southern California. Est., Coast. Shelf Sci. 58, 25–40.

Foveau, A., Desroy, N., Le Mao, P., 2018. Contrôle de surveillance benthique de la Directive Cadre sur l'Eau (2000/60/CE): Volume II: Flore autre que phytoplancton, Année 2016. District Seine-Normandie. 145pp.

Fox, C.H., Paquet, P.C., Reimchen, T.E., 2015. Novel species interactions: american black bears respond to Pacific herring spawn. BMC Ecol. 15, 14.

Fraser, C.I., Morrison, A.K., Hogg, A.M., Macaya, E.C., van Sebille, E., Ryan, P.G., Padovan, A., Jack, C., Valdivia, N.C., Waters, J.M., 2018. Antarticta's ecological isolation will be broken by storm-driven dispersal and warming. Nat. Clim. Change. 8, 704-708.

Garden, C.J., Smith, A.M., 2015. Voyages of seaweeds: The role of macroalgae in sediment transport. Sediment. Geol. 318, 1-9.

Gómez, M., Barreiro, F., López, J., Lastra, M., de la Huz, R., 2013. Deposition patterns of algal wrack species on estuarine beaches. Aquat. Bot. 105, 25-33.

Guiry MD, Guiry GM (2020) AlgaeBase. World-wide electronic publication, National University of Ireland, Galway. https://www. algaebase.org; last accessed on 17 January 2020.

Kroeze, C., Hofstra, N., Ivens, W., Löhr, A., Strokal, M., van Wijnen, J., 2013. The links between global carbon, water and nutrient cycles in an urbanizing world — the case of coastal eutrophication. Curr. Opin. Environ. Sustainability 5, 566-572.

Lastra, M., Rodil, I.F., Sánchez-Mata, A., García-Gallego, M., Mora, J., 2014. Fate and processing of macroalgal wrack subsidies in beaches of Deception Island, Antarctic Peninsula. J. Sea Res. 88, 1-10.

López, B.A., Macaya, E.C., Tala, F., Tellier, F., Thiel, M., 2017. The variable routes of rafting: stranding dynamics of floating bull kelp *Durvillaea antarctica* (Fucales, Phaeophyceae) on beaches in the SE Pacific. J. Phycol. 53, 70-84.

López, B.A., Macaya, E.C., Jeldres, R., Valvidia, N., Bonta C.C., Tala, F., Thiel, M., 2019. Spatio-temporal variability of strandings of the southern bull kelp *Durvillaea antarctica* (Fucales, Phaeophyceae) on beaches along the coast of Chile – linked to local storms. J. Appl. Phycol. 31, 2159-2173.

Liu, D., Keesing, J.K., He, P., Wang, Z., Shi, Y., Wang, Y., 2013. The world's largest macroalgal bloom in the Yellow Sea, China: Formation and implications. Est. Coast. Shelf Est. 129, 2-10.

MacLachlan, A., Brown, A.C., 2006. The ecology of sandy shores. Academic Press, Burlington, MA.

Mandalka, A., Cavalcanti, M.I.L.G., Fujii, M.T., Eisner, P., Schweiggert-Weisz, U., Chow, F., 2022. Nutritional composition of beach-cast marine algae biomass considered as waste. Foods 11, 1201-1220.

Mellbrand, K., Lavery, P.S., Hyndes, G., Hambäck, P.A., 2011. Linking land and sea: different pathways for marine subsidies. Ecosystems 14, 732-744.

Merceron, M., Antoine, V., Auby, I., Morand, P., 2007. *In situ* growth potential of the subtidal part of green tide forming *Ulva* spp. stocks. Sci. Total Environ. 384, 293-305.

559 Morand, P., Briand, X., 1996. Excessive growth of macroalgae: A symptom of environmental
560 disturbance. Bot. Mar. 39, 491-516.

561 Ochieng C.A., Erftemeijer P.L A., 1999. Accumulation of seagrass beach cast along the Kenyan coast: a
562 quantitative assessment. Aquat. Bot. 65, 221–238.

563 Orr, M., Zimmer, M., Jelinsky, D.E., Mews, M., 2005. Wrack deposition on different beach types: spatial
564 and temporal variation in the pattern of subsidy. Ecology 86, 1496-1507.

565 Orr, K.K., Wilding, T.A., Horstmeyer, L., Weigl, S., Heymans, J.J., 2014. Detached macroalgae: Its
566 importance to inshore sandy beach fauna. Est. Coast. Shelf Sci. 150, 125-135.

567 Panayotidis, P., Montesanto, B., Orfanidis, S., 2004. Use of low-budget monitoring of macroalgae to
568 implement the European Water Framework Directive. J. Appl. Phycol. 16, 49-59.

569 Perrot, T., Rossi, N., Ménesguen, A., Dumas, F., 2014. Modelling green macroalgal blooms on the coasts
570 of Brittany, France to enhance water quality management. J. Mar. Syst. 132, 38–53.

571 Piriz, M.L., Eyras, M.C., Rostagno, C.M., 2003. Changes in biomass and botanical composition of beach-
572 cast seaweeds in a disturbed coastal area from Argentine Patagonia. J. Appl. Phycol. 15, 67-74.

573 Ren, J.S., Barr, N.G., Scheuer, K., Schiel, D.R., Zeldis, J., 2014. A dynamic growth model of macroalgae:
574 Application in an estuary recovering from treated wastewater and earthquake-driven eutrophication.
575 Est. Coast. Shelf Sci. 148, 59-69.

576 Rivier, A., Gohin, F., Bryère, P., Petus, C., Guillou, N., Chapalain, G., 2012. Observed vs. predicted
577 variability in non-algal suspended particulate matter concentration in the English Channel in relation
578 to tides and waves. Geo-Mar. Lett. 32,139-151.

579 Schreiber, L., Lopez, B.A., Rivadeneira, M.M., Thiel, M., 2020. Connections between benthic
580 populations and local strandings of the southern bull kelp *Durvillaea antarctica* along the continental
581 coast of Chile. J. Phycol. 56, 185-197.

582 Schreyers, L., van Emmerik, T., Biermann, L., Le Lay, Y-F., 2021. Spotting green tides over Brittany from
583 space: Three decades of monitoring with landsat imagery. Remote Sens. 13, 1408-1422.

584 Suursaar, Ü., Torn, K., Martin, G., Herkül, K., Kullas, T. 2014. Formation and species composition of
585 stormcast beach wrack in the Gulf of Riga, Baltic Sea. Oceanologia 56, 673-695.

586 Thakur, M.C., Reddy, C.R.K., Jha, B., 2008. Seasonal variation in biomass and species composition of
587 seaweeds stranded along Port Okha, northwest coast of India. J. Earth Syst. Sci. 117, 211-218.

588 Teichberg, M., Fox, S.E., Olsen, Y.S., Valiela, I., Martinetto, P., Iribarne, O., Muto, E.Y., Petti, M.A.V.,
589 Corbisier, T.N., Soto-Jiménez, M., Paez-Osuna, F., Castro, P., Freitas, H., Zitelli, A., Cardinaletti, M.,
590 Tagliapietra, D., 2010. Eutrophication and macroalgal blooms in temperate and tropical coastal waters:
591 nutrient enrichment experiments with *Ulva* spp. Glob. Chang. Biol. 16, 2624-2637.

592 Van der Molen, J., Bolding, K., Greenwood, N., Mills, D.K., 2009. A 1-D vertical multiple grain size model
593 of suspended particulate matter in combined currents and waves in shelf seas. J. Geophys. Res. 114.
594 doi:10.1029/2008JF001150

595 Villares, R., Fernández-Lema, E., López-Mosquera, M.E., 2016. Evaluation of beach wrack for use as an
596 organic fertilizer: Temporal survey in different areas. Thalassas 32, 19-36.

Figure captions

Figure 1: Temporal change in (A) mean area of beach substrate covered by wrack (Ha) and (B) mean biomass of wrack (kg fresh wt.m^{-2}) measured in the study area (30 Ha). The shaded interval represents one standard deviation around the mean (N=6 quadrats).

Figure 2: Percentage of each taxon stranded relative to the monthly mean cover. Only species with a total mean cover >2% throughout the sampling period are considered.

Figure 3: Temporal variation of macroalgae coverage (A) and of species richness (B) determined on the rocky shore of Luc-sur-Mer (histograms represent the mean +SD of three replicates). Different letters indicate significant differences between seasons.

Figure 4: Pie chart of the percentage of each functional group of seaweeds observed in the wrack deposits and on the rocky shore for the whole sampling period.

Figure 5: Seaweed beaching events observed from June to October 2017, and from August to October 2018 grouped in 4 classes (Negligible: < 1 Ha; Small: between 1 and 2.5 Ha; Moderate: between 2.5 and 4.5 Ha; Large: > 4.5 Ha) along with the forecast tide height (m) and associated wind speed (m s^{-1}).

Figure 6: A) Wind rose plot of wind speed (m.s^{-1}) and direction frequencies recorded at the Bernières-sur-Mer meteorological station during the growing seasons (spring and summer) in 2017 and 2018. Wind speeds are split into four intervals. (B) and (C) Pollution roses showing which wind directions contributed the most to the different levels of (B) SWH (m) and (C) Algal wrack surface area (Ha) (Negligible: < 1 Ha; Small: between 1 and 2.5 Ha; Moderate: between 2.5 and 4.5 Ha; Large: > 4.5 Ha). The levels are defined as the four quantiles. The grey circles show the frequencies in the three plots.

Table captions

Table 1: List of species identified in seaweed beachings and on the rocky shore at Luc-sur-Mer in spring, summer, autumn and winter 2017 and 2018. A number links each seaweed species to its functional group (1: Crustose; 2: Filamentous; 3: Foliose; 3,5: Corticated foliose; 4: "Corticated", thick, soft; 4,5: "Corticated", thick, hard; 5: Leathery; 6: Calcareous) according to Blomqvist et al. (2014).

Table 2: PERMANOVA results based on Bray-Curtis dissimilarities of square root-root transformed data testing the effects of the factors "Extent of algal wrack", "Year" and "Month" on the seaweed assemblages of beach wrack (77 variables). P values were obtained using 999 permutations of permutable units.

Table 3: Spearman correlations (r) between the extent of algal wrack deposits and the physical and meteorological variables (the maximum tidal current (TCmax in $m.s^{-1}$), the median value of the significant wave height (SWH in m) and the mean wind speed ($m.s^{-1}$) measured 24 hours before the stranding event and the median daily value of air temperature and solar radiation on the 3 days preceding sampling). Significant Spearman correlations are in bold. *p-value < 0.05; **p-value < 0.01; ***p-value < 0.001.

Table 4: Average percentage of days in a month with more than 1300 J/cm^2 or 15°C at the Bernières-sur-Mer weather station.

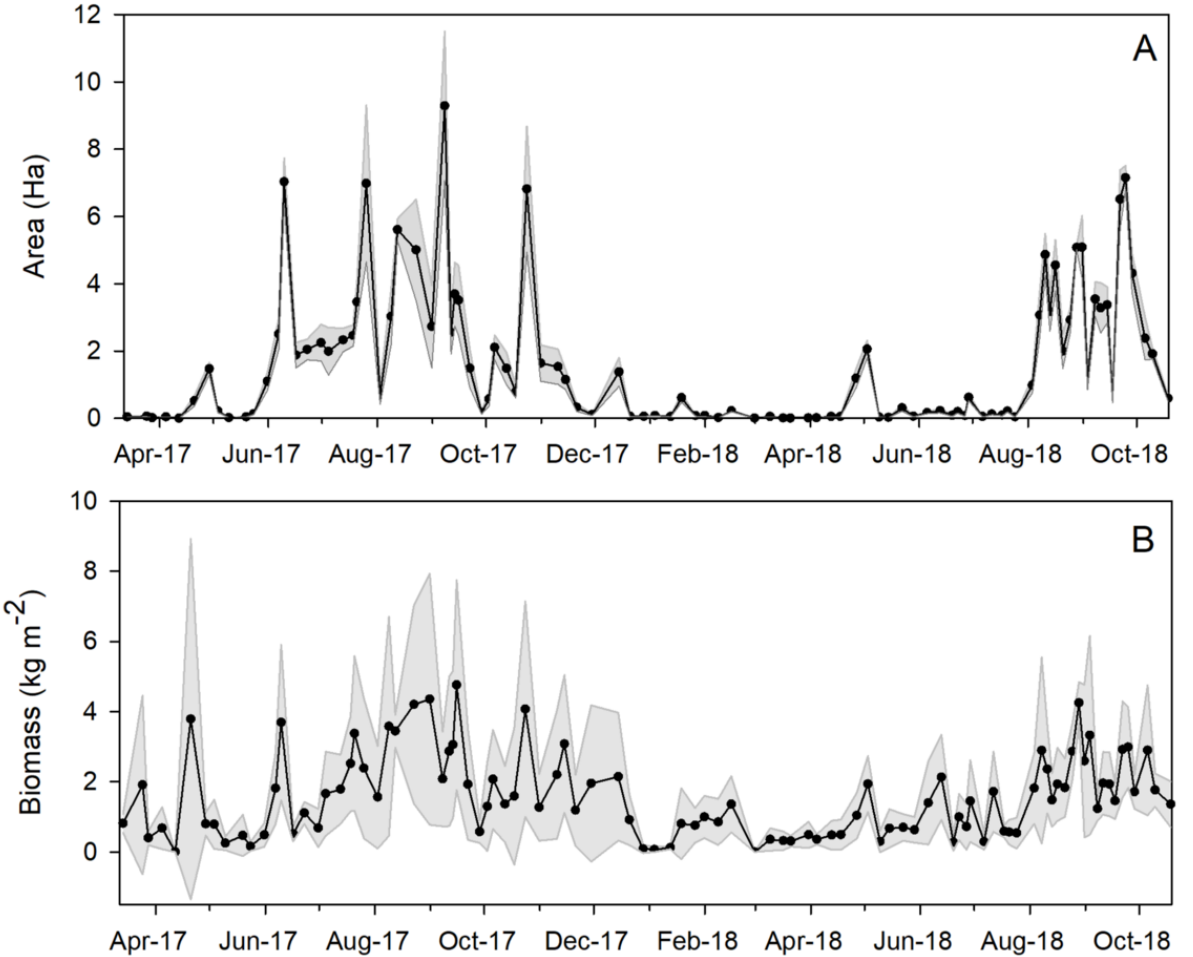
A
Area (Ha)
0
2
4
6
8
10
12
Apr-17
Jun-17
Aug-17
Oct-17
Dec-17
Feb-18
Apr-18
Jun-18
Aug-18
Oct-18
B
Biomass (kg m-2)
0
2
4
6
8
10
Apr-17
Jun-17
Aug-17
Oct-17
Dec-17
Feb-18
Apr-18
Jun-18
Aug-18
Oct-18

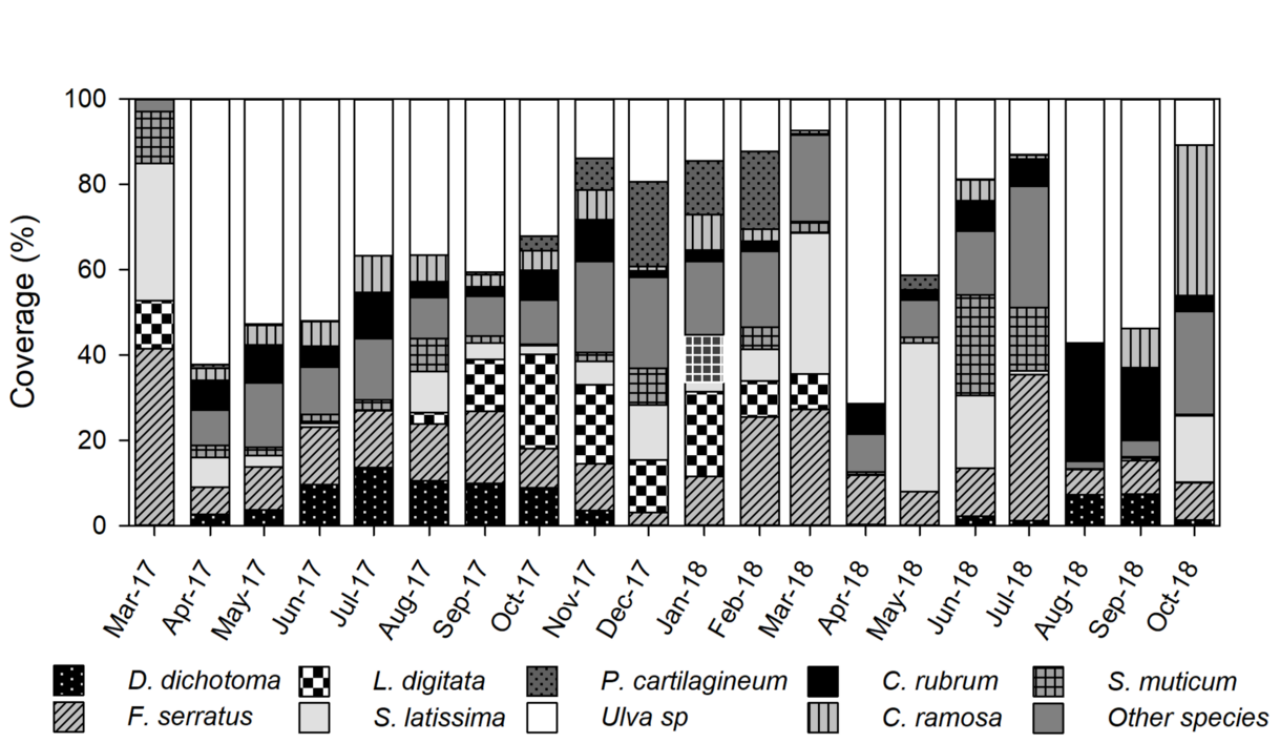
Coverage (%)
100
80
60
40
20
0
Mar-17
Apr-17
May-17
Jun-17
Jul-17
Aug-17
Sep-17
Oct-17
Nov-17
Dec-17
Jan-18
Feb-18
Mar-18
Apr-18
May-18
Jun-18
Jul-18
Aug-18
Sep-18
Oct-18
D. dichotoma
F. serratus
L. digitata
S. latissima
P. cartilagineum
Ulva sp
C. rubrum
C. ramosa
S. muticum
Other species

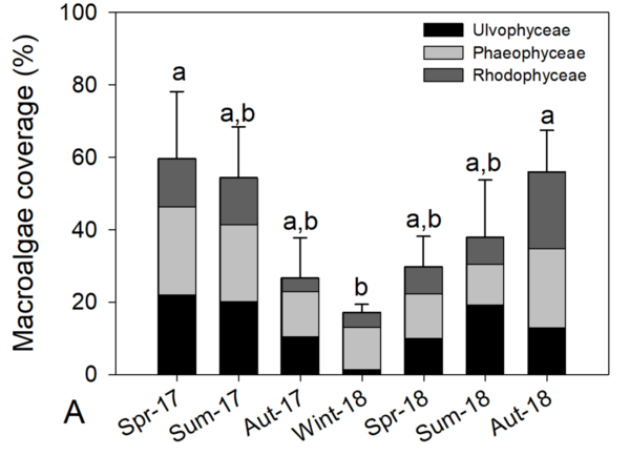
Macroalgae coverage (%)
100
80
60
40
20
0
Ulvophyceae
Phaeophyceae
Rhodophyceae
a
a,b
a,b
b
a,b
a,b
a
Spr-17
Sum-17
Aut-17
Wint-18
Spr-18
Sum-18
Aut-18
A

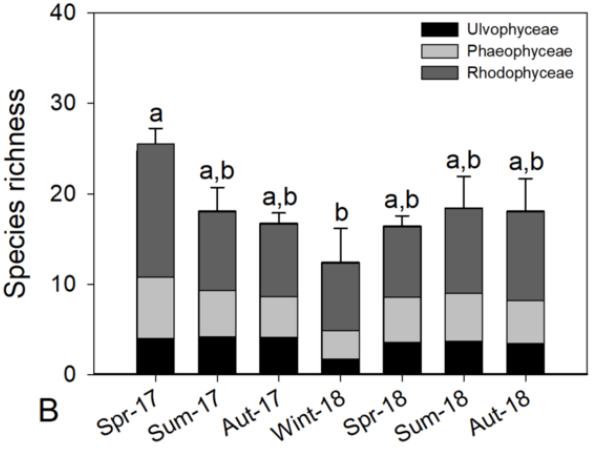
Species richness
40
30
20
10
0
Ulvophyceae
Phaeophyceae
Rhodophyceae
a
a,b
a,b
b
a,b
a,b
a,b
Spr-17
Sum-17
Aut-17
Wint-18
Spr-18
Sum-18
Aut-18
B

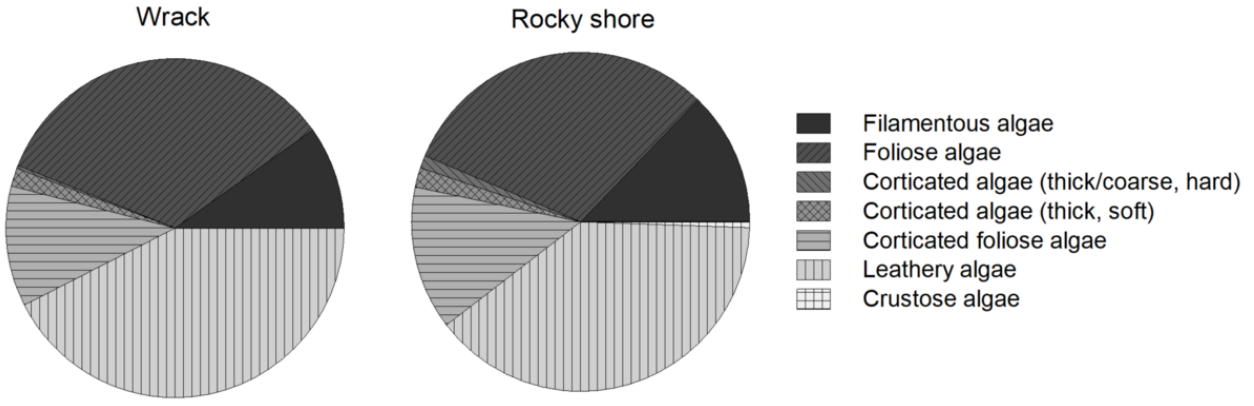
Wrack
Rocky shore
Filamentous algae
Foliose algae
Corticated algae (thick/coarse, hard)
Corticated algae (thick, soft)
Corticated foliose algae
Leathery algae
Crustose algae

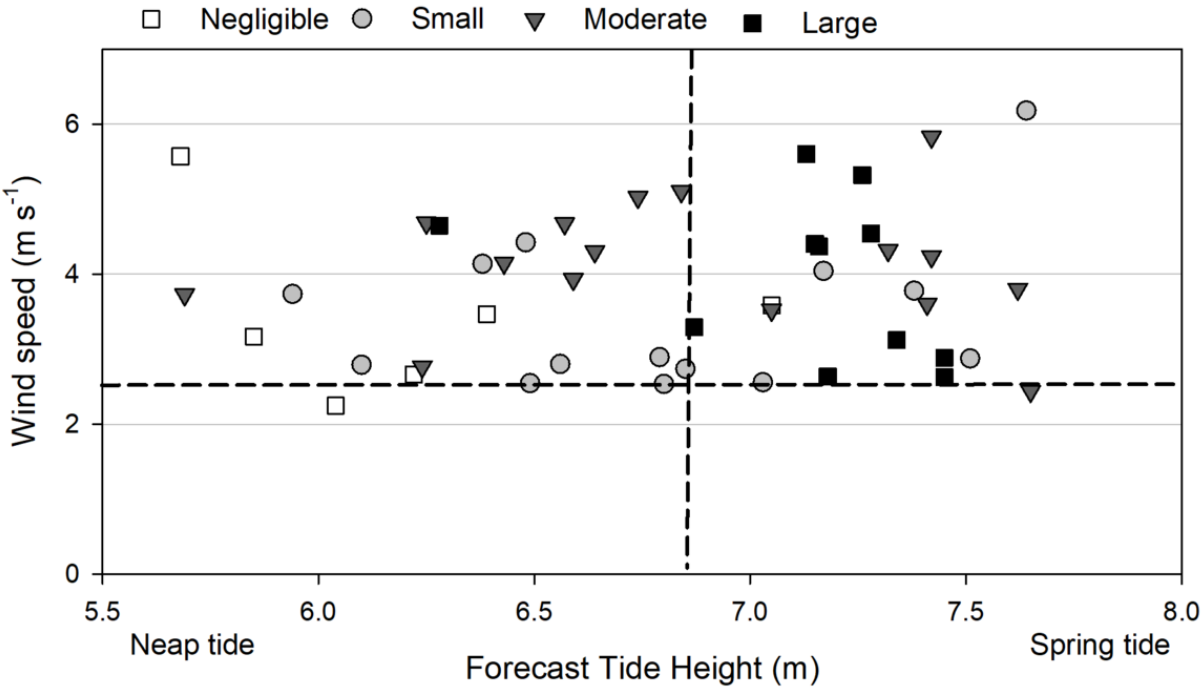
Negligible
Small
Moderate
Large
Wind speed (m s-1)
0
2
4
6
5.5
6.0
6.5
7.0
7.5
8.0
Neap tide
Spring tide
Forecast Tide Height (m)

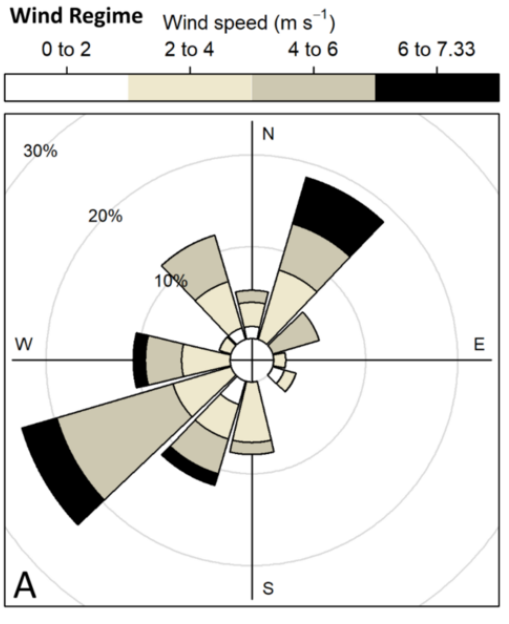

Frequency of counts by wind direction (%)

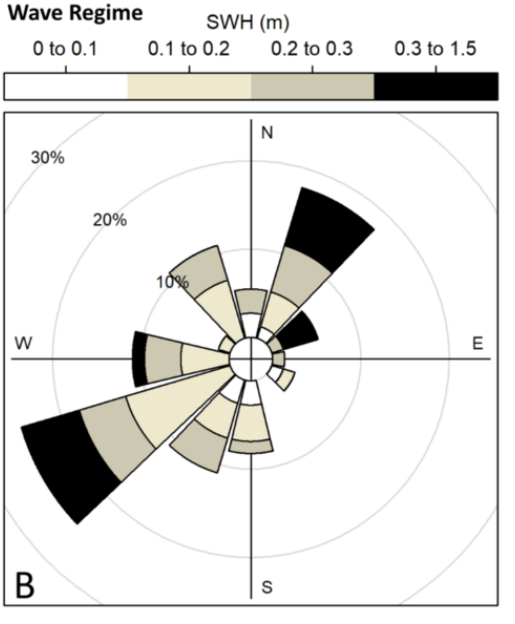

Frequency of counts by wind direction (%)

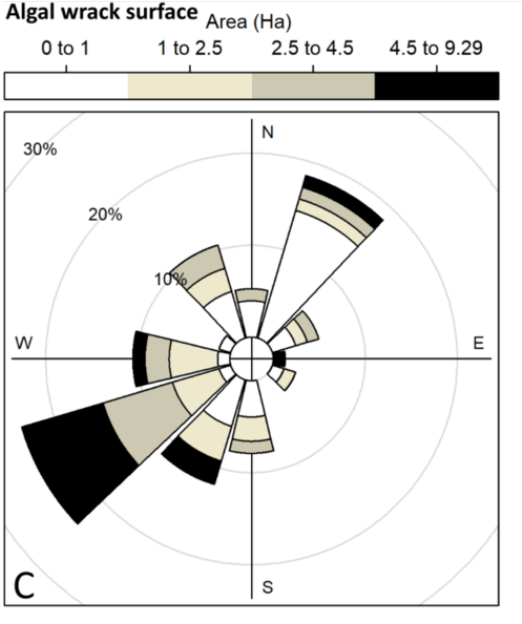

Frequency of counts by wind direction (%)

		Beach Wrack (BW)							Rocky shore (RS)								
	Functional group	**Sp-17**	**Su-17**	**Au-17**	**Wi-18**	**Sp-18**	**Su-18**	**Au-18**	**Sp-17**	**Su-17**	**Au-17**	**Wi-18**	**Sp-18**	**Su-18**	**Au-18**	RS	BW
Phaeophyta																	
Ascophyllum nodosum	5			X			X										X
Cladostephus spongiosus	4				X	X											X
Desmarestia ligulata	5		X														X
Dictyota dichotoma	3.5	X	X	X		X	X	X	X	X	X			X	X	X	X
Ectocarpales	2	X				X	X	X	X	X	X		X		X	X	X
Fucus serratus	5	X	X	X	X	X	X	X	X	X	X	X	X	X	X	X	X
Fucus vesiculosus	5	X	X	X	X	X	X	X	X	X	X		X	X		X	X
Halidrys siliquosa	5		X	X	X												X
Himanthalia elongata	5			X		X	X										X
Laminaria digitata	5	X	X	X	X		X	X	X							X	X
Saccharina latissima	5	X	X	X	X	X	X	X	X	X	X	X	X	X	X	X	X
Sargassum muticum	5	X	X	X	X	X	X	X	X	X	X	X	X	X	X	X	X
Scytosiphon lomentaria	4					X		X									X
Taonia atomaria	3.5						X							X	X	X	X
Rhodophyta																	
Antithamnionella ternifolia	2						X								X	X	X
Apoglossum ruscifolium	3.5		X	X	X	X											X
Calliblepharis ciliata	3.5	X	X	X													X
Callophyllis laciniata	3.5	X	X	X	X	X	X	X									X
Ceramium rubrum	2	X	X	X	X	X	X	X	X	X	X	X	X	X	X	X	X
Chondria coerulescens	2		X						X	X	X			X		X	X
Chondria dasyphylla	2	X	X	X		X	X		X	X			X	X	X	X	X
Chondria scintillans	2			X													X
Chondrus crispus	3.5	X	X	X	X	X	X	X	X	X	X	X	X	X	X	X	X
Corallina sp.	6			X													X
Cryptopleura ramosa	3.5	X	X	X	X	X	X	X	X		X	X		X	X	X	X
Cystoclonium purpureum	4	X	X	X	X	X	X		X	X	X	X	X	X	X	X	X
Dasya corymbifera	2			XX		X											X
Dilsea carnosa	3.5	X	X	X	X	X	X	X	X	X	X	X	X	X	X	X	X
Gracilaria bursa-pastoris	4.5								X							X	
Gracilaria gracilis	4.5		X	X		X	X	X	X	X	X	X	X	X	X	X	X
Halurus flosculosus	2								X	X				X		X	
Hildenbrandia rubra	1								X	X		X			X	X	
Lithophyllum incrustans	1								X		X	X	X	X	X	X	
Lithothamnion lenormandii	1								X	X	X	X	X	X	X	X	
Heterosiphonia plumosa	2	X	X	X	X	X	X	X									X
Hypoglossum hypoglossoides	3.5	X		X													X
Kallymenia reniformis	3.5			X	X	X											X
Nitophyllum punctatum	3.5								X						X	X	
Palmaria palmata	3.5	X	X	X	X	X	X		X	X	X	X	X	X		X	X
Plocamium cartilagineum	2	X	X	X	X	X	X				XX	X			X	X	X
Plumaria elegans	2	X	X	X	X	X	X		X					X		X	X
Polyides rotundus	4.5				X	X											X
Polysiphonia fucoides	2		X						X	X						X	X
Polysiphonia nigrescens	2	X															X
Porphyra sp.	3	X	X	X		X	X	X	X	X	X			X	X	X	X
Rhodophyllis divaricata	3.5					X	X	X					X	X		X	X
Rhodothamniella floridula	2						X		X	X	X	X		X		X	X
Scinaia furcellata	4		X							X						X	X
Chlorophyta																	
Cladophora laetevirens	2		X						X							X	X
Ulva intestinalis	3	X	X	X		X	X		X	X	X		X	X	X	X	X
Ulva sp	3	X	X	X	X	X	X	X	X	X	X	X	X	X	X	X	X
Ulva compressa	3	X	X	X		X			X	X	X		X	X	X	X	X
Umbraulva olivascens	3		X		X												X

Factors	Df	SS	MS	F	P
Extent of algal wrack	1	1.035	1.035	13.45	**0.001**
Month	11	3.537	0.322	4.18	**0.001**
Year	1	0.308	0.308	4.00	**0.003**
Month :Year	7	1.390	0.199	2.58	**0.001**
Residuals	56	4.309	0.077		

	Algal wrack surface (all sampling period)	Algal wrack surface (Spring/Summer)
Air temperature	**0,52*** **	**0,42*** **
Solar Radiation	0,09	**-0,24***
Wind speed	0,002	0,14
Maximum Tidal Current	0,04	0,01
Significant Wave Height	0,17	**0,27***

Months		**Jan.**	**Feb.**	**Mar.**	**Apr.**	**May**	**Jun.**	**Jul.**	**Aug.**	**Sept.**	**Oct.**
Solar Radiation	**2017**	0%	0%	16%	**83%**	74%	90%	71%	74%	23%	3%
>1300 J/cm²	**2018**	0%	0%	6%	**47%**	90%	73%	94%	61%	73%	13%
Air Temperature	**2017**	0%	0%	10%	3%	**45%**	83%	100%	97%	57%	35%
>15°C	**2018**	0%	0%	0%	10%	**19%**	70%	100%	100%	70%	32%